

## Effects of Nb, Ti and V on recrystallization kinetics of austenite in microalloyed steels

**M. Opiela\*, W. Ozgowicz**

Division of Constructional and Special Materials,  
Institute of Engineering Materials and Biomaterials,  
Silesian University of Technology, ul. Konarskiego 18a, 44-100 Gliwice, Poland

\* Corresponding e-mail address: marek.opiela@polsl.pl

Received 14.10.2012; published in revised form 01.12.2012

### Manufacturing and processing

#### ABSTRACT

**Purpose:** The work presents research results of impact of Nb, Ti and V microadditions on flow stress, recrystallization kinetics and microstructure of newly elaborated steels assigned for production of forged machine parts, using the method of thermo-mechanical treatment.

**Design/methodology/approach:** The study was performed with the use of Gleeble 3800 simulator. Stress-strain curves were determined during continuous compression test in a temperature range from 900 to 1100°C and at a strain rate of 1, 10 and 50 s<sup>-1</sup>. In order to determine recrystallization kinetics of plastically deformed austenite, discontinuous compression tests of specimens were done with a given strain at the rate of 10 s<sup>-1</sup>, in a temperature range from 900 to 1100°C, with isothermal holding of samples between successive stages of deformation for 2 to 100 s. Recrystallization kinetics of plastically deformed austenite was described using the Johnson-Mehl-Avrami equation. The observations of microstructures of thin foils were done using JEOL JEM 3010 transmission electron microscope.

**Findings:** Basing on the analysis of the form and the course of curves obtained in the compression test, it was found that in the studied range of parameters of hot plastic deformation, the decrease of strain hardening of studied steels is caused by the process of continuous dynamic recrystallization. This is also confirmed by calculation results of activation energy of plastic deformation process. Performed two-stages compression tests revealed that microadditions introduced into steel considerably influence the kinetics of static recrystallization.

**Research limitations/implications:** It was found that the time necessary for a total course of recrystallization of austenite is too long to be accepted in the production process of forgings.

**Practical implications:** Executed hot compression tests will contribute to establishing conditions of forging with the method of thermo-mechanical treatment.

**Originality/value:** Strain-stress curves and recrystallization kinetics curves of newly elaborated microalloyed steels have been determined.

**Keywords:** Microalloyed steel; Thermo-mechanical treatment; Dynamic recrystallization; Static recrystallization; Softening kinetics

#### Reference to this paper should be given in the following way:

M. Opiela, W. Ozgowicz, Effects of Nb, Ti and V on recrystallization kinetics of austenite in microalloyed steels, Journal of Achievements in Materials and Manufacturing Engineering 55/2 (2012) 759-771.

## 1. Introduction

Die forging is a commonly used method of production of machine parts obtained from unalloyed and alloy steels. Forged parts of unalloyed steels are usually subjected to normalizing. However, alloy steel parts forged prior to mechanical working require application of soft annealing or high-temperature tempering, and in a final state - toughening and dimensional correction with the methods of machining processes, i.e. machine cutting or grinding. The pursuit of lower production cost is a basis for implementation of economical technologies of products made of constructional alloy steels with the methods of thermo-mechanical treatment. These methods consist in plastic working conducted in conditions adjusted to their chemical composition and the type of introduced microadditions with consecutive direct hardening of parts from the temperature of plastic deformation finish or after particular time specified. This allows reducing expensive heat treatment of products exclusively to tempering. Desired mechanical and technological properties, i.e. high yield strength at guaranteed crack resistance, can be obtained for metallurgical products with fine-grained microstructure [1-6].

HSLA-type (High Strength Low Alloy) microalloyed steels - containing up to 0.3% C and 2% Mn and microadditions with high chemical affinity to N and C, i.e. Nb, Ti and V in the amount of about 0.1%, and sometimes also slightly increased concentration of N and up to 0.005% of B, increasing hardenability - are particularly useful for production of forged parts with fine-grained microstructure using the method of thermo-mechanical processing. The interaction of microadditions in steel in a solid state depends on their state under conditions of performed plastic working. Microadditions dissolved in a solid solution raise the temperature of recrystallization of plastically deformed austenite as a result of segregation on dislocations and grain boundaries, causing decrease of recovery rate and mobility of grain boundaries. Instead, microadditions precipitating on dislocations in the form of dispersive particles of MX interstitial phases, slow down the course of dynamic recovery and possibly also dynamic recrystallization during the plastic deformation and additionally decrease the rate of thermal recovery and static or metadynamic recrystallization and limit grain growth of recrystallized austenite in the intervals between successive stages of deformation and after its finish [7-10].

The impact of concentration of several elements, dissolved in a solid solution or bounded in dispersive carbide particles, on the course of thermal recovery and static recrystallization of austenite at the temperature of 1000 and 900°C of steel consisting of 0.05% C, 1.2% Mn and 0.3% Si, after hot deformation with a rate of  $2 \text{ s}^{-1}$ , is presented in Fig. 1. Segments of lines with small slope to the time axis, running from the beginning of the system, correspond with the course of static recovery. The remaining parts of kinetic curves describe the course of static recrystallization. Comparison of these curves indicates that the decrease of plastic strain temperature and decrease of isothermal holding temperature from 1000 to 900°C causes considerable extension of recovery time and decrease of austenite recrystallization rate. In case of presented steel, at the temperature of 1000°C, Mo and partially V can be found in austenite in a dissolved state. In comparison with Mo and V, stronger influence on decreasing the rate of the course of these two thermally activated processes, is exerted by Nb,

which prevailing part at this temperature is bounded in dispersive NbC carbide particles formed on dislocations in plastically deformed austenite. The strongest impact on increasing the time of recovery and recrystallization is caused by contribution of segregation of dissolved atoms and dispersive carbides, which applies to steels containing Nb and V, and in particular, containing Mo, Nb and V (Fig. 1a). The  $t_{0.5}$  time necessary to form 50% fraction of austenite recrystallized at such temperature of steel with basic composition is equal approximately 1.5 s and increases up to 80 s when adding Mo, Nb and V in a given concentration, and the time of complete recrystallization of austenite increases even more, from about 20 to 2000 s. Broken lines marked in the figure define the probable course of the kinetic curves without the influence of dispersive carbide particles. Inhibiting impact of alloying constituents introduced into steel on the course of recovery and static recrystallization of austenite is particularly effectively noted after decreasing the temperature of plastic deformation and the temperature of isothermal holding to 900°C (Fig. 1b).

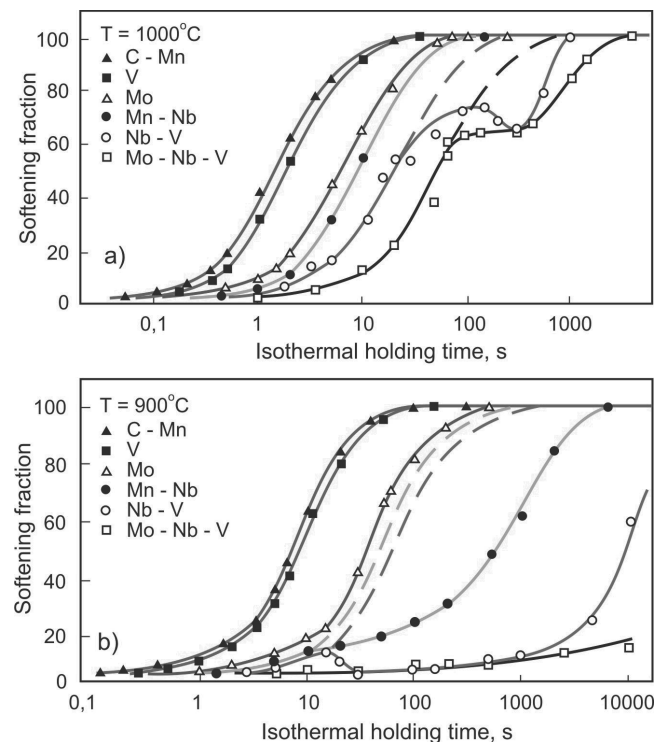


Fig. 1. Influence of the Mo (0.3%), Nb (0.035%) and V (0.115%) content on the recovery and recrystallization kinetics of steel containing 0.05% C, 1.2% Mn and 0.3% Si after hot-working with a strain rate of  $2 \text{ s}^{-1}$  [11,12]: a - at a temperature of 1000°C, b - at a temperature of 900°C

At such temperature, Mo and a slight portion of introduced V can be found in a solid solution in dissolved state. Nb and the remaining part of V are bounded into NbC and VC or  $\text{V}_4\text{C}_3$  carbides, respectively. In this case, the  $t_{0.5}$  time of austenite of steel with base composition is equal approximately 9 s and increases up to about  $10^4$  s when microadditions of Nb and V are

introduced into steel. The grade of decay of strain hardening of austenite of steel with addition of Mo, Nb and V, caused by the recovery and static recrystallization at the temperature of 900°C after mentioned time of soaking, is equal only 20% [11].

Given data have a considerable significance in designing the technology of hot-working of steels, especially micro-alloyed steels, with methods of thermo-mechanical treatment. In addition, performed analysis indicates that apart from the temperature, considerable influence on recovery and static recrystallization kinetics is exerted by chemical and phase composition of steel. The  $t_R$  time of total recrystallization of alloy and unalloyed steels containing microadditions of elements with high chemical affinity for carbon and nitrogen, bounded in dispersive particles of carbides, carbonitrides or nitrides at recrystallization temperature, may be long. For that reason, the  $t_{0.5}$  has a greater significance for technical purpose than  $t_R$  time [13,14].

The analysis of numerous scientific works carried out by Sellars [15] concerning the course of austenite recrystallization of steel containing from 0.055 to 0.68% C and from 0.46 to 0.85% Mn revealed that in the range of strain lower than necessary to initiate dynamic recrystallization ( $\epsilon < 0.8\epsilon_m$ ) the time for half recrystallization of austenite is described with the following model dependence:

$$t_{0.5} = 2.5 \cdot 10^{-19} \cdot d_0^2 \cdot \epsilon^{-4} \exp(300000/RT), \quad (1)$$

and at higher deformations:

$$t_{0.5} = 1.06 \cdot 10^{-5} \cdot Z^{-6} \exp(300000/RT), \quad (2)$$

where:  $d_0$  - initial grain size of austenite,  $Z$  - Zener-Hollomon parameter,  $R$  - gas constant,  $T$  - temperature.

While the model dependence, elaborated in the same work, determining the  $t_{0.5}$  time of austenite of steel containing from 0.05 to 0.42% C, from 0.71 to 1.5% Mn and Nb microaddition at a concentration of 0.04%, is as follows:

$$t_{0.5} = 2.52 \cdot 10^{-19} \cdot d_0^2 \cdot \epsilon^{-4} \exp(325000/RT), \quad (3)$$

for  $\epsilon < \epsilon_{cd}$  and  $T > 1000^\circ\text{C}$ ,

$$t_{0.5} = 5.94 \cdot 10^{-38} \cdot d_0^2 \cdot \epsilon^{-4} \exp(780000/RT), \quad (4)$$

for  $\epsilon < \epsilon_{cd}$  and  $1000^\circ\text{C} > T > 890^\circ\text{C}$  and

$$t_{0.5} = 9.24 \cdot 10^{-9} \cdot d_0^2 \cdot \epsilon^{-4} \exp(130000/RT), \quad (5)$$

for  $\epsilon < \epsilon_{cd}$  and  $T < 890^\circ\text{C}$ .

## 2. Material and methodology

The research was performed on newly elaborated microalloyed steels. Chemical composition of steel (Table 1) was designed taking into consideration the production of forged machine elements with energy-saving method of thermo-mechanical processing.

Table 1.  
Chemical composition of the investigated steels

Alloying	Mass contents, (%)	
	Steel A	Steel B
C	0.31	0.28
Mn	1.45	1.41
Si	0.30	0.29
P	0.006	0.008
S	0.004	0.004
Cr	0.26	0.26
Ni	0.11	0.11
Mo	0.22	0.22
Nb	—	0.027
Ti	0.033	0.028
V	0.008	0.019
B	0.003	0.003
Cu	0.20	0.20
Al	0.040	0.025
N	0.0043	0.0039
O	0.0006	0.0006

Molten steels are characterized with high metallurgical purity, i.e. they have limited concentration of P and S impurities and gases.

Investigated steel melts, weighing 100 kg, were done in VSG-100 type laboratory vacuum induction furnace, produced by PVA TePla AG. Furnace charge consisted of ARMCO, 04JA grade iron and alloy additions, mainly in the form of pure metals (Mn, Cr, Ni, Mo, Cu, Ti and Al) and ferroalloys (FeV, FeNb and FeB) as well as non-metallic additions (C and Si). In order to modify non-metallic inclusions, mischmetal (~50% Ce, ~20% La, ~20% Nd) in the amount of 2g/kg of steel was used. Casting was performed in atmosphere of argon through heated intermediate ladle to quadratic section cast iron hot-topped ingot mould: top - 160/mm bottom - 140 mm x 640 mm. In order to obtain 32x160 mm flat bars, initial hot-working of ingots was performed implementing the method of open die forging in high-speed hydraulic press, produced by Kawazoe, applying 300 MN of force. Heating of ingots to forging was conducted in gas forging furnace. The range of forging temperature was equal 1200-900°C, with interoperation reheating in order to prevent the temperature of the material to drop below 900°C. Ingot bodies were subjected to forging without feedheads which were cut off during forging.

In order to determine the effect of temperature and strain rate as well as time of isothermal holding between two stages of deformation on changes of flow stress, strain hardening and degree of softening, plastometric tests were carried out with the use of Gleeble 3800 device, allowing to compress specimens according to established program. Axisymmetrical samples with 10 mm in diameter and 12 mm in length were used for the purpose of research. Continuous compression tests of samples up to true strain equal  $\epsilon=1$  were performed in order to obtain  $\sigma$ - $\epsilon$  curves and activation energy of plastic deformation. Specimens were resistance heated in vacuum at a rate of 3°C/s to a temperature of 1150°C, where the austenite grain size was about

100 and 80  $\mu\text{m}$  - for the steels A and B respectively. The samples were held at 1150°C for 30 s and cooled to deformation temperature equal 1100, 1050, 1000, 950 and 900°C. Compression of specimens was realized at a strain rate of 1, 10 and 50  $\text{s}^{-1}$ . In order to minimize the effect of friction on the flow curves tantalum foils were used to prevent sticking and graphite foils as a lubricant. Additionally, both surfaces were covered with nickel-based substance. Smoothing procedure using Origin software was used to obtain  $\sigma$ - $\varepsilon$  curves. A correction procedure taking into account the effect of adiabatic heating on flow stress values is in progress.

Activation energy of the process of plastic deformation was calculated with the use of Energy 4.0 program, basing on the following dependence:

$$\dot{\varepsilon} = A[\sinh(\alpha\sigma)]^n \exp(-Q/RT), \quad (6)$$

where: A,  $\alpha$ , n - constants,  $\dot{\varepsilon}$  - strain rate, T - strain temperature, Q - activation energy of the process of plastic deformation, R = 8.314  $\text{J mol}^{-1} \text{K}^{-1}$  - gas constant,  $\sigma$  - value of stress corresponding with the maximum value of flow stress.

Part of samples subjected to true strain equal 0.2, 0.4 and 0.8 was cooled in water in order to freeze their microstructure and to identify processes which control the course of strain hardening. So as to determine kinetics of recrystallization of plastically deformed austenite, discontinuous compression tests of samples were performed in a temperature range from 900 to 1100°C with isothermal holding of specimens between successive deformations for 2 to 100 s. The softening kinetics was determined according to the following dependence:

$$X = (\sigma_1 - \sigma_2) / (\sigma_1 - \sigma_0) \quad (7)$$

where:  $\sigma_0$  and  $\sigma_1$  - the stress necessary to initiate plastic strain and its value at the moment of its finish in the first stage of deformation, respectively,  $\sigma_2$  - the stress necessary to initiate plastic deformation in the second stage of deformation after  $\Delta t$  time between those stages.

Recrystallization kinetics of plastically deformed austenite was described with the use of the Johnson-Mehl-Avrami equation:

$$y = 1 - \exp(-k \cdot t^n) \quad (8)$$

where: y - fraction of recrystallized austenite after t time, k - constant, n - index exponent. Time  $t_{0.5}$  corresponding to 50% recrystallized austenite was assessed on the basis of experimentally determined Avrami-type relationship.

In order to reveal grains of primary austenite, metallographic observations of samples cooled in water directly after applied strain value and successive etching of metallographic specimens was conducted in OPTON, AXIOVERT 405M light microscope, with magnification ranging from 100 to 800x. Metallographic specimens were prepared according to axis of a sample, in a distance of 1/3 of radius from the centre of sample. The observations of microstructures of thin foils were done using JEOL JEM 3010 transmission electron microscope, at the accelerating voltage equal 300 kV.

### 3. Results

The analysis of the process of hot plastic deformation of the A and B steels conducted in the temperature range from 900 to 1100°C and at the strain rate of 1, 10 and 50  $\text{s}^{-1}$ , allowed to define the impact of compression parameters at constant temperature of austenitizing equal 1150°C, on the shape of work-hardening curves, determined in the function of flow stress  $\sigma$  - strain  $\varepsilon$ .

The work-hardening curves for the A and B steels obtained in the studied temperature range and strain rate are characterized with similar shape and their course (Figs. 2-4). In the initial stage of compression, substantial increase of yield stress, as a result of increasing density of dislocations generated in this process, can be observed on the work-hardening curves in the range of strain  $\varepsilon < 0.1$ . In the next stage of compression, at strain increased from  $\varepsilon=0.1$  to  $\varepsilon=\varepsilon_m$ , slight increase of stress takes place until the maximum value of flow stress is attained. This indicates that thermally activated processes, causing partial decay of emitted dislocations, occur along with formation of new dislocations during the plastic deformation. For the strain equal  $\varepsilon_m < \varepsilon < \varepsilon=1.0$ , work-hardening curves are characterized with gentle decrease of flow stress to the value of state equilibrium between processes of strain hardening and its decrease in the consequence of the course of thermally activated processes.

In the considered range of temperature and strain rate, compression curves of the B steel are characterized with slightly higher values of maximum flow stress  $\sigma_m$  in comparison to the A steel. It's a result of deformation of primary austenite grains of the A and B steel, diversified in respect of chemical composition and size, after austenitizing at the temperature of 1150°C. The A steel after austenitizing at the temperature of 1150°C and compression at 900°C is characterized with grains of  $\gamma$  phase with average diameter ranging from 40 to 75  $\mu\text{m}$  (Fig. 5), and the B steel with austenite grains with sizes ranging from 20 to 55  $\mu\text{m}$  (Fig. 6). Finer-grained microstructure of austenite in the B steel is a result of the presence of NbC carbides, essentially inhibiting the growth of  $\gamma$  phase grains. Additionally, it can be stated that smaller amount of potential areas for nucleation of dynamic recrystallization, i.e. primary grain boundaries, near-boundary areas and twin boundaries, is noted in case of coarse-grained microstructures of austenite when comparing to fine-grained microstructures. It leads to formation of bigger subgrains and, in consequence, to the lower values of flow stress in hot deformed steel.

Similar values of stress on the work-hardening curves, obtained during compression at the temperature of 900°C at the strain rate of 1 and 50  $\text{s}^{-1}$  (Fig. 4) and during compression at the temperature of 1100°C at the strain rate of 10  $\text{s}^{-1}$  and 50  $\text{s}^{-1}$  are observed for both investigated steels. Along with decrease of temperature and increase of strain rate, the values of  $\varepsilon_m$  strain, complying with the maximum value of flow stress, move towards higher deformations. For the strain rate of 1  $\text{s}^{-1}$ , decrease of temperature of deformation from 1100 to 900°C leads to the increase of maximum flow stress from 98 MPa to 186 MPa and their movement from  $\varepsilon_m=0.262$  to  $\varepsilon_m=0.415$  for the A steel, and increase of  $\sigma_m$  from 103 MPa to 192 MPa and their movement towards higher deformations - from  $\varepsilon_m=0.274$  to  $\varepsilon_m=0.425$  for the B steel. Decrease of strain temperature in the same range during compression at the rate of 50  $\text{s}^{-1}$  influences the increase of  $\sigma_m$

from 169 MPa to 285 MPa for the A steel and from 173 MPa to 285 MPa for the B steel. For described parameters of compression,  $\epsilon_m$  strain increases from  $\epsilon_m=0.371$  to  $\epsilon_m=0.568$  for the A steel and from  $\epsilon_m=0.435$  to  $\epsilon_m=0.590$  for the B steel.

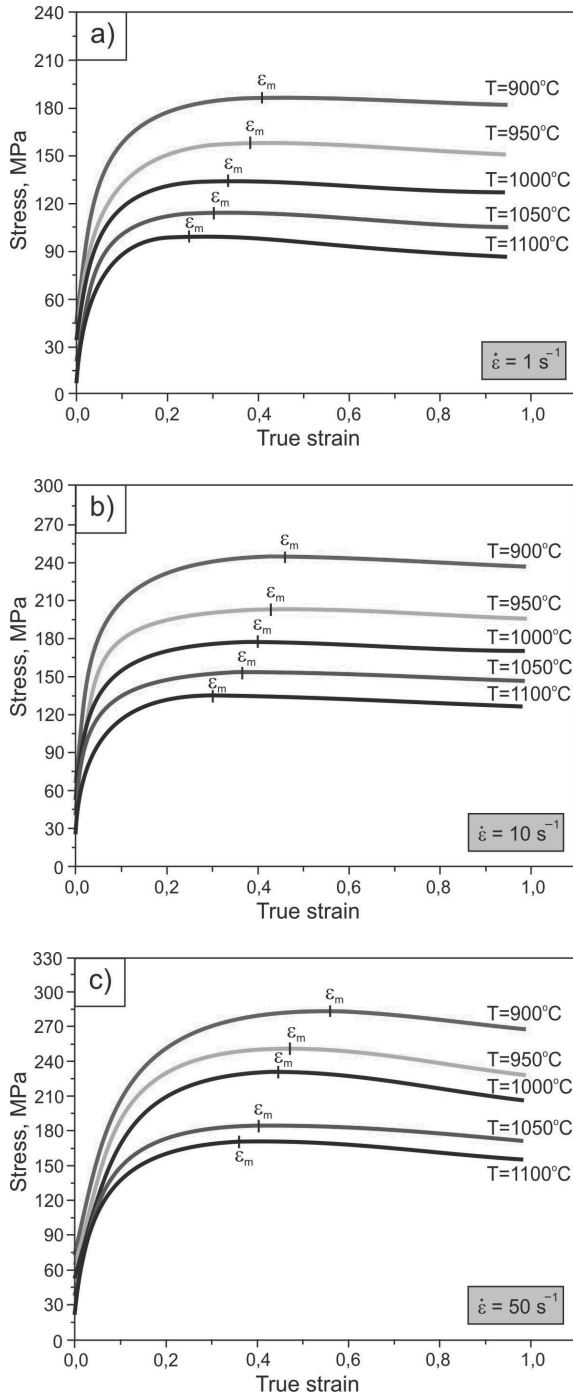


Fig. 2. Influence of the plastic deformation temperature and strain rate (a-c) on a shape of  $\sigma$ - $\epsilon$  curves for the steel A subjected to continuous compression test

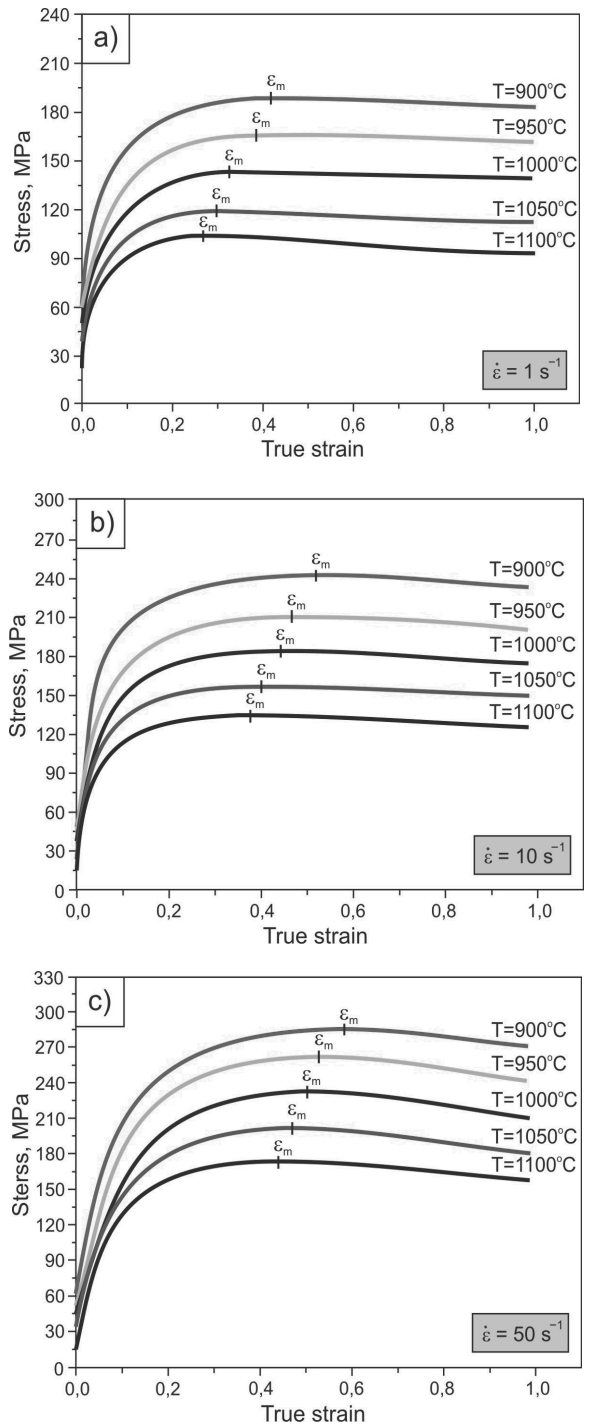


Fig. 3. Influence of the plastic deformation temperature and strain rate (a-c) on a shape of  $\sigma$ - $\epsilon$  curves for the steel B subjected to continuous compression test

During compression of the A steel at the rate of  $10 \text{ s}^{-1}$  at the temperature of  $900^\circ\text{C}$  the value of  $\sigma_m$  is equal 245 MPa and takes

place at the strain equal  $\varepsilon_m = 0.458$ , and in case of the B steel - value of  $\sigma_m = 246$  MPa at  $\varepsilon_m = 0.527$ . Increase of strain rate up to the temperature of  $1100^\circ\text{C}$  at the strain rate of  $10\text{ s}^{-1}$  causes a decrease of  $\sigma_m$  to the value of 124 MPa in case of the A steel, and to the value of 134 MPa in case of the B steel. The values of  $\varepsilon_m$  corresponding with maximum flow stress are equal 0.302 and 0.384 - for the A and B steel, respectively. Detailed data

concerning the conditions and results obtained in the continuous compression test are set together in Table 2.

The analysis of the form and the shape of curves obtained in the compression test allows to state that in the studied range of hot plastic deformation parameters, the decrease of strain hardening, both in case of the A and B steel, is caused by the process of continuous dynamic recrystallization.

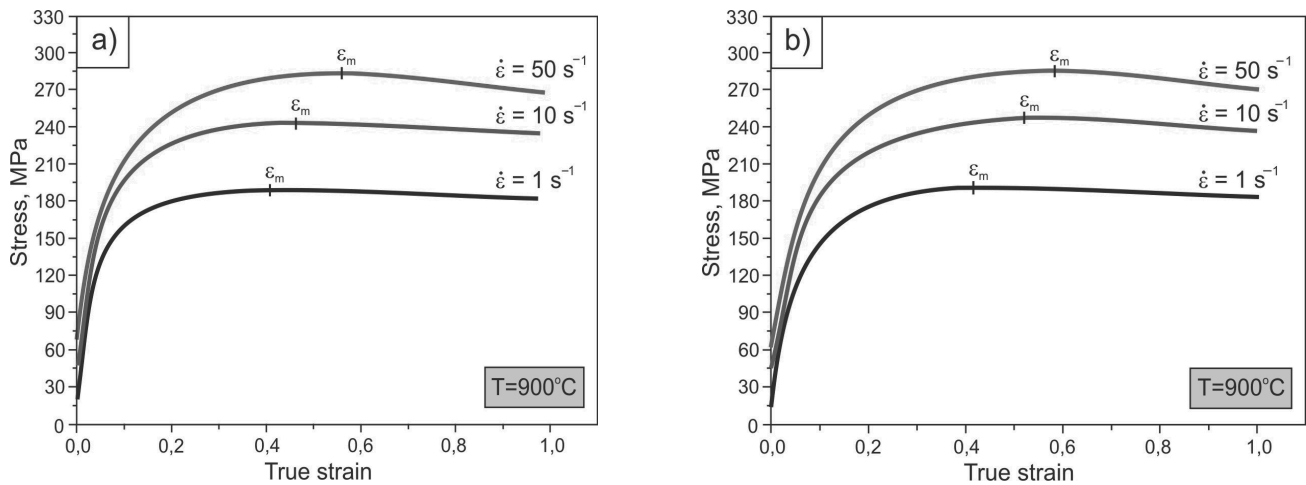


Fig. 4. Influence of the strain rate on a shape  $\sigma$ - $\varepsilon$  curves for the steel A (a) and steel B (b) subjected to continuous compression test at a temperature of  $900^\circ\text{C}$

Table 2.

Results of the continuous compression of specimens

No	Temperature of plastic deformation, $^\circ\text{C}$	$\dot{\varepsilon}$ , $\text{s}^{-1}$	Steel A		Steel B	
			Maximum strain $\varepsilon_m$	Maximum stress $\sigma_m$ , MPa	Maximum strain $\varepsilon_m$	Maximum stress $\sigma_m$ , MPa
1	900	1	0.415	186.2	0.425	191.9
2	950	1	0.381	157.5	0.390	165.0
3	1000	1	0.336	135.0	0.338	144.7
4	1050	1	0.307	114.4	0.309	118.8
5	1100	1	0.262	98.60	0.274	103.7
6	900	10	0.458	244.8	0.527	246.2
7	950	10	0.428	201.5	0.469	210.0
8	1000	10	0.409	177.3	0.438	185.1
9	1050	10	0.368	153.9	0.405	157.5
10	1100	10	0.302	124.7	0.384	133.8
11	900	50	0.568	285.0	0.590	285.1
12	950	50	0.483	250.5	0.536	262.6
13	1000	50	0.454	232.7	0.507	234.4
14	1050	50	0.409	184.8	0.472	198.8
15	1100	50	0.371	169.5	0.435	173.0

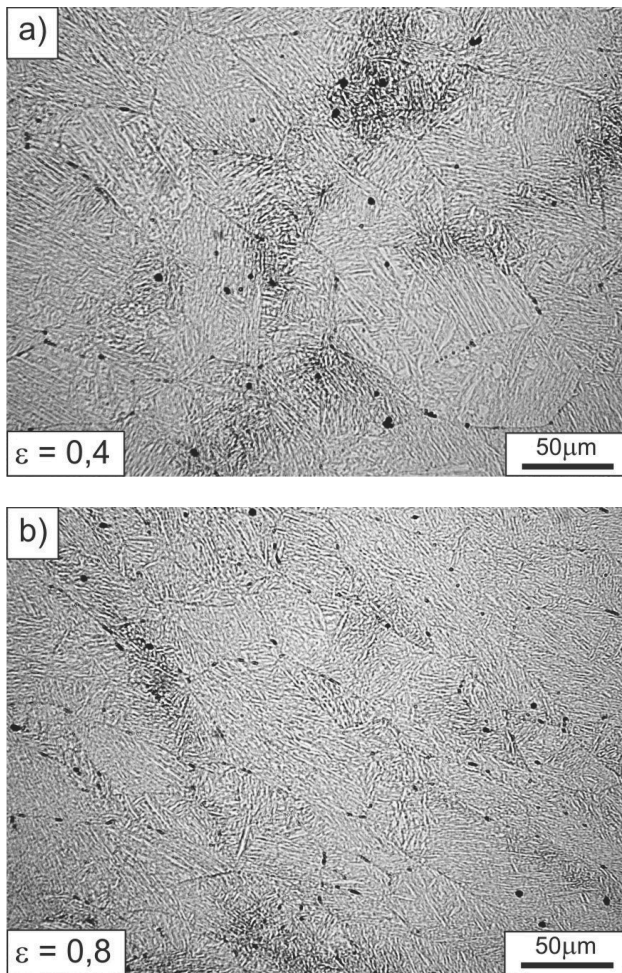


Fig. 5. Primary austenite structures of steel A quenched in water from a temperature of 900°C after the true strain  $\varepsilon=0.4$  (a) and  $\varepsilon=0.8$  (b) with the strain rate  $10s^{-1}$

This is also confirmed by the results of evaluation of activation energy of plastic deformation process of examined steel. Activation energy of plastic deformation of the A steel, determined with the use of equation (6), is equal  $Q = 382.48 \text{ kJ}\cdot\text{mol}^{-1}$ , while activation energy of plastic deformation process of the B steel is equal  $Q = 397.95 \text{ kJ}\cdot\text{mol}^{-1}$ , wherein values of constants in this equation for the stress corresponding with  $\varepsilon_m$  deformations are equal:  $A = 3.43 \cdot 10^{15}$ ,  $\alpha = 0.00628$ ,  $n = 6.93$  and  $A = 7.42 \cdot 10^{15}$ ,  $\alpha = 0.00649$ ,  $n = 7.17$  - for the A and B steel, respectively. Values of activation energy of hot-working obtained for investigated steels are substantially higher than activation energy of self-diffusion (creep), when the processes which control the course of plastic deformation are dislocation climbing and formation of subgrains. It means, that the process of plastic deformation of the A and B steels is controlled by dynamic recrystallization.

The research of thin foils in transmission electron microscope revealed that the A steel hardened from the temperature of 900°C has a lath morphology of dislocation martensite with numerous

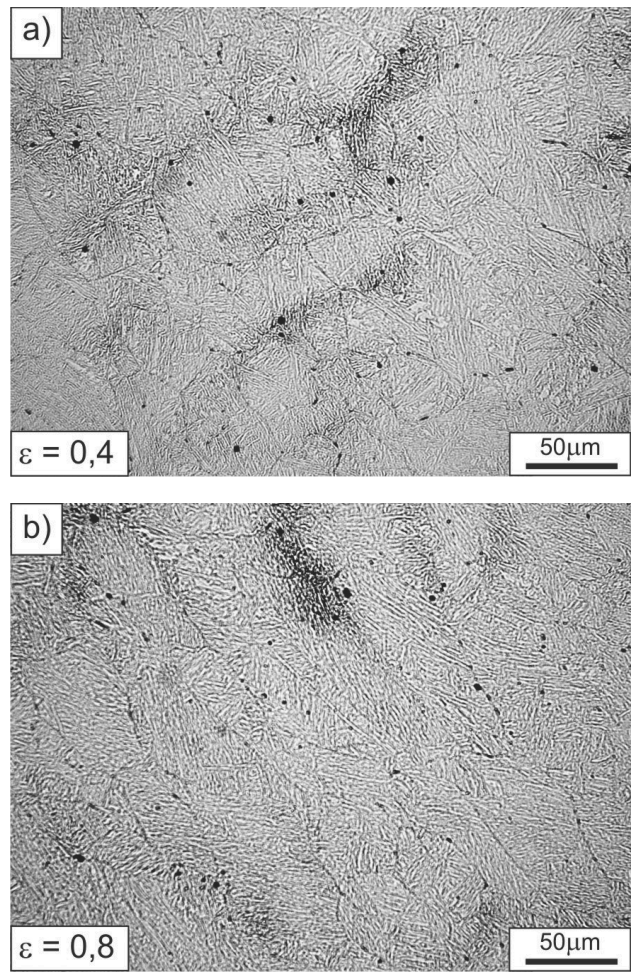


Fig. 6. Primary austenite structures of steel B quenched in water from a temperature of 900°C after the true strain  $\varepsilon=0.4$  (a) and  $\varepsilon=0.8$  (b) with the strain rate  $10s^{-1}$

twinning after true strain of 0.2, 0.4 and 0.8 (Figs. 7, 8). Martensite exhibits bent laths with jogs as a result of interaction of non-uniform distribution of dislocation density in plastically deformed austenite. Presence of dispersive particles of cementite (Fig. 9), formed in the process of self-tempering, was revealed with the method of electron diffraction in martensite with diversified orientation of particular laths. Self-tempering processes of austenite were confirmed through revealing Bagariacki's crystallographic dependence between cementite precipitations and martensitic matrix. In addition, the presence of retained austenite distributed in the form of thin films between laths of martensite, was also revealed in microstructure of investigated steel. Kurdjumow-Sachs crystallographic dependence was found between retained austenite and martensite. Moreover, TiC carbides were revealed in the A steel martensite (Fig. 10).

The B steel presents similar morphology of lath martensite, hardened under the same conditions, as the A steel. Laths with different width and quite diversified orientation around specific crystal zone are present in the packets of martensite. Some of the

laths reveal fragmentation (Fig. 11) and some others, curvilinear grain boundaries and variable width. Dispersive precipitations of  $\text{Fe}_3\text{C}$  with privileged orientation with matrix, formed in the self-tempering process of the  $\alpha$  supersaturated solid solution, are present in B steel martensite, similarly as in case of the A steel. Additionally, the presence of dispersive NbC carbides was also revealed in the B steel martensite (Fig. 12).

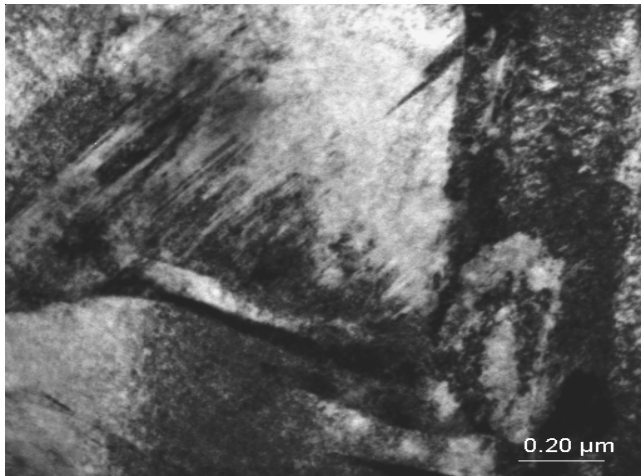


Fig. 7. Twinned martensite in a centre part of the lath; (steel A,  $\epsilon=0.4$ )

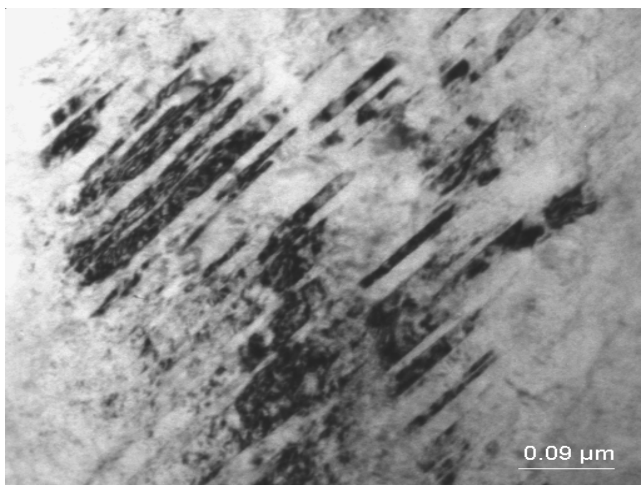


Fig. 8. Twinned martensite structure; (steel A,  $\epsilon=0.8$ )

Conducted research of recrystallization of the A and B steel after two-stage hot compression allowed to determine the influence of testing temperature on the kinetics of thermally activated processes. Discontinuous compression tests of specimens at given strain revealed, according to expectations, that there is a partial and even complete decay of strain hardening between two stages of deformation, depending on the strain temperature and the time of isothermal holding. Research results of strain hardening kinetics of studied steels are set together in Table 3.

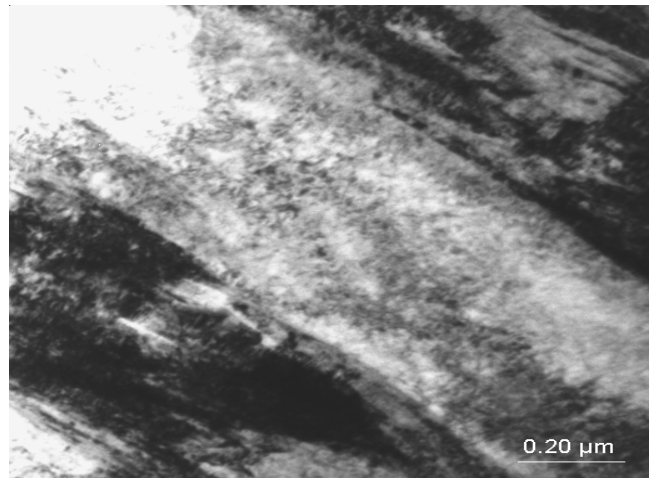


Fig. 9. Lath martensite structure with the dispersive cementite precipitations inside the laths; (steel A,  $\epsilon=0.8$ )

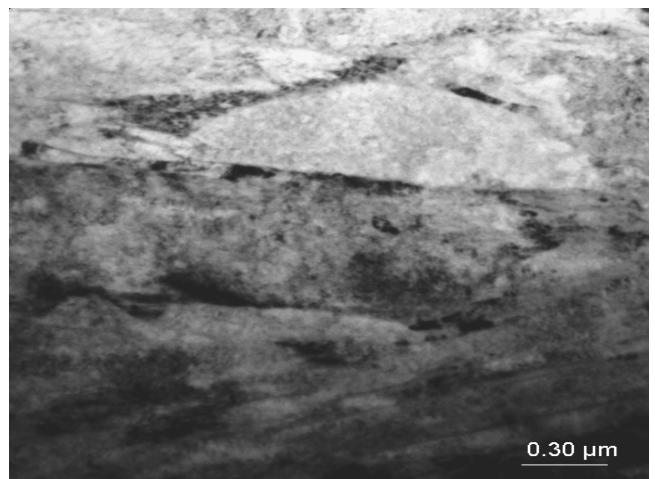


Fig. 10. Lath martensite structure with TiC dispersive precipitations (steel A,  $\epsilon=0.4$ )

The impact of alloying elements, dissolved in a solid solution and the presence of dispersive particles of MX-type interstitial phases on a rate of recovery and mobility of recrystallization front, significantly influences kinetics of static recrystallization of studied steels. This interaction is illustrated as strain hardening curves of the A steel austenite containing 0.31% C, 1.45% Mn, 0.22% Mo and microadditions of Ti and V in the amount of 0.033% and 0.008%, respectively (Fig. 13a). Comparison of the course of softening kinetics curves for the A steel indicates that the decrease of plastic deformation temperature and decrease of isothermal holding temperature from 1100 to 900°C causes considerable extension of recovery time and decrease of austenite recrystallization rate.



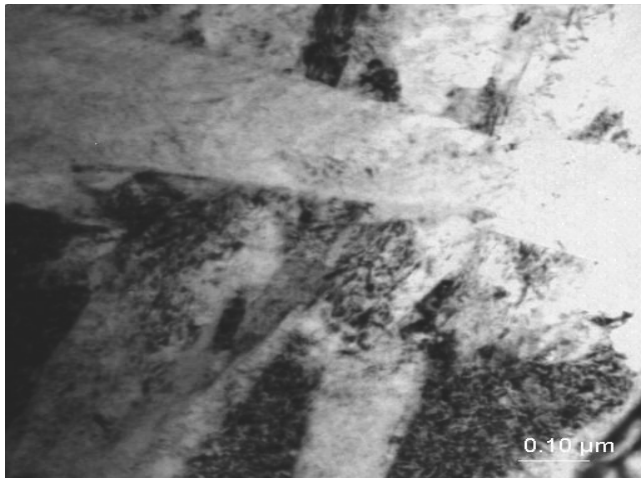
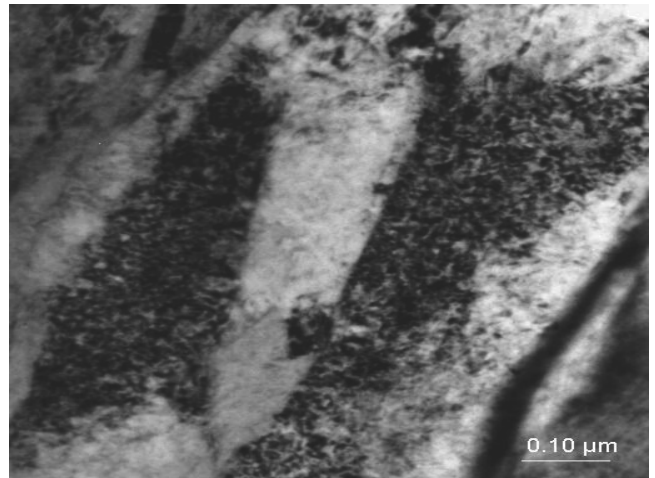

 Fig. 11. Lath martensite structure (steel B,  $\epsilon=0.8$ )

 Fig. 12. Lath martensite structure with NbC dispersive precipitations; (steel B,  $\epsilon=0.8$ )

 Table 3.  
 Results of the discontinuous compression of specimens

Steel designation	Temperature of plastic deformation, °C	$\dot{\epsilon}$ , $s^{-1}$	$\epsilon_1$	Isothermal holding time, s	$\epsilon_2$	$\sigma_0$ MPa	$\sigma_1$ MPa	$\sigma_2$ MPa	Softening fraction X
steel A	900	10	0.2	2	0.2	143.22	224.02	212.20	0.15
			0.2	5	0.2	153.91	214.74	201.18	0.22
			0.2	10	0.2	154.71	215.06	195.30	0.32
			0.2	50	0.2	153.99	217.34	177.43	0.63
			0.2	100	0.2	157.40	211.46	166.60	0.83
	1000	10	0.2	2	0.2	109.51	165.62	152.52	0.23
			0.2	5	0.2	110.30	164.32	147.04	0.32
			0.2	10	0.2	110.01	165.55	137.35	0.50
			0.2	50	0.2	109.50	163.32	117.84	0.84
			0.2	100	0.2	112.11	166.23	114.99	0.95
	1100	10	0.2	2	0.2	87.64	122.20	112.54	0.28
			0.2	5	0.2	87.36	123.25	105.31	0.49
			0.2	10	0.2	87.24	123.74	98.65	0.68
			0.2	50	0.2	79.91	115.97	82.73	0.92
			0.2	100	0.2	79.29	119.32	79.29	1.00
steel B	900	10	0.2	2	0.2	138.64	219.11	214.34	0.06
			0.2	5	0.2	139.32	220.46	210.19	0.12
			0.2	10	0.2	138.68	218.70	205.63	0.16
			0.2	50	0.2	141.49	220.51	187.80	0.41
			0.2	100	0.2	161.81	221.77	180.55	0.68
	1000	10	0.2	2	0.2	108.76	165.05	156.00	0.17
			0.2	5	0.2	108.00	167.01	150.15	0.28
			0.2	10	0.2	109.93	161.27	142.39	0.37
			0.2	50	0.2	108.40	161.76	123.51	0.72
			0.2	100	0.2	108.42	162.85	117.41	0.83
	1100	10	0.2	2	0.2	95.81	125.14	117.86	0.24
			0.2	5	0.2	95.86	123.79	112.55	0.40
			0.2	10	0.2	95.42	124.24	106.08	0.63
			0.2	50	0.2	95.69	123.77	100.49	0.83
			0.2	100	0.2	93.98	121.94	95.04	0.96

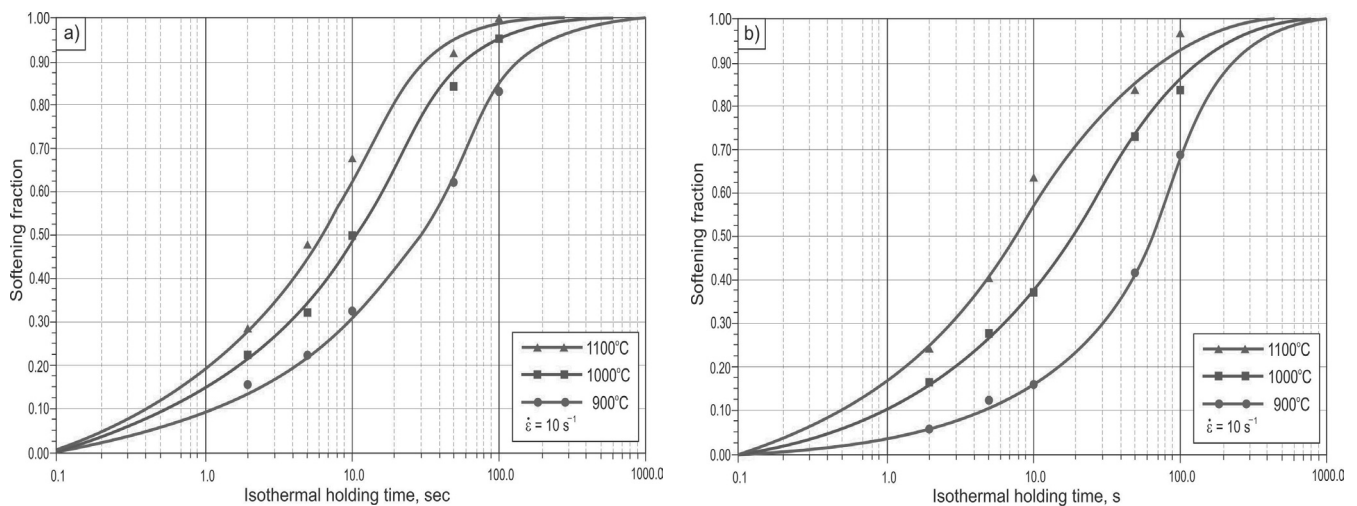


Fig. 13. Effect of the test temperature on the softening fraction of deformed austenite for the steel A (a) and steel B (b)

It's a result of decreasing value of self-diffusion coefficient of Fe and coefficients of volume diffusion of alloying constituents along with lowering the temperature as well as influence of their atoms and dispersive particles of interstitial phases of microadditions introduced into steel on the migration rate of recrystallization fronts. In case of the A steel, Mo and V and partially Ti can be found in austenite at the temperature of 1100°C in dissolved state. Interaction of dissolved elements leads to elongation of recovery time and decrease of recrystallization rate due to segregation of those atoms in the deformation field of dislocations and on recrystallization fronts, causing decrease of their mobility. The greatest influence on elongation of times of recovery and recrystallization is exerted by contribution of segregation of dissolved atoms and dispersive particles of interstitial phases. As shown in Fig. 13a, the time  $t_{0.5}$  necessary to form 50% fraction of recrystallized austenite at the temperature of 1100°C is equal approximately 6 s and increases to about 30 s together with decrease of the compression temperature to 900°C. Time of total recrystallization of austenite,  $t_R$ , which varies from 100 to about 600 s in investigated temperature range, drags even more.

Strain hardening curves for the B steel containing 0.28% C, 1.41% Mn, 0.22% Mo and microadditions of Nb, Ti and V in the amount of 0.027% and 0.028% and 0.019%, respectively, are presented in Fig. 13b. Data shown in the figure indicates that inhibiting interaction of alloying elements introduced into steel on the course of recovery and static recrystallization of austenite is particularly effectively noted after decreasing the temperature of plastic deformation and the temperature of isothermal holding to 900°C. At this temperature, there is Mo and microaddition of vanadium present in a solid solution in dissolved state. In turn, microadditions of Nb and Ti are completely bounded into NbC, TiN and TiC at this temperature.

The shape of analyzed kinetic curves indicates the possibility of describing them in accordance with the model of recrystallization after hot deformation, taking into consideration the process of static recovery, metadynamic recrystallization and static recrystallization. Contribution of metadynamic recrystallization to the decrease of strain hardening after

deformation of the A steel, realized at the temperature of 1100°C, at the rate of  $1 \text{ s}^{-1}$ , is possible because of applied value of strain equal  $\varepsilon=0.2$ , close to the  $\varepsilon_{cd}$  value, required for initiation of dynamic recrystallization. Applied degree of deformation, at lower strain temperature and at higher strain rates, was lower than required for initiation of the process of dynamic recrystallization. Nevertheless, after deformation of the A steel at the temperature of 900°C, at the rate of  $10 \text{ s}^{-1}$ , decrease of strain hardening is caused by the process of static recovery and static recrystallization, and at the temperature of 1000 and 1100°C - by the process of static recovery, metadynamic recrystallization and static recrystallization. Whereas, in the B steel, deformed at the temperature of 900 and 1000°C, the decrease of strain hardening is a result of the course of static recovery and static recrystallization, and deformed at 1100°C, it's controlled by the course of metadynamic and static recrystallization.

Furthermore, conducted discontinuous compression tests of investigated steels in the two-stage deformation applying isothermal holding for the time ranging from 2 to 100 s revealed that kinetics curves of recrystallization of plastically deformed austenite of the B steel are clearly displaced towards right in relation to kinetics curves of plastically deformed austenite of the A steel. It should be explained with interaction of Nb microaddition, which presence in the B steel has a great influence on the decrease of rate of thermally activated processes. The beginning of precipitation of NbC carbides for equilibrium conditions occurs at the temperature of about 1135°C [16]. It means, that certain portion of niobium is bounded into dispersive particles of NbC carbides, formed on dislocations in plastically deformed austenite, already at the temperature of 1100°C. The fraction of NbC carbides in a solid solution increases along with temperature decrease, and niobium is bounded into NbC at the temperature of 900°C.

Experimentally determined values of the  $t_{0.5}$  time for the A steel reveal good correspondence with the model equation for C-Mn-V steel, written as:

$$t_{0.5} = 6.767 \cdot 10^{-10} \cdot \varepsilon^{-2} \cdot \dot{\varepsilon}^{-0.46} \cdot d_0 \cdot \exp(166000/RT) \quad (9)$$

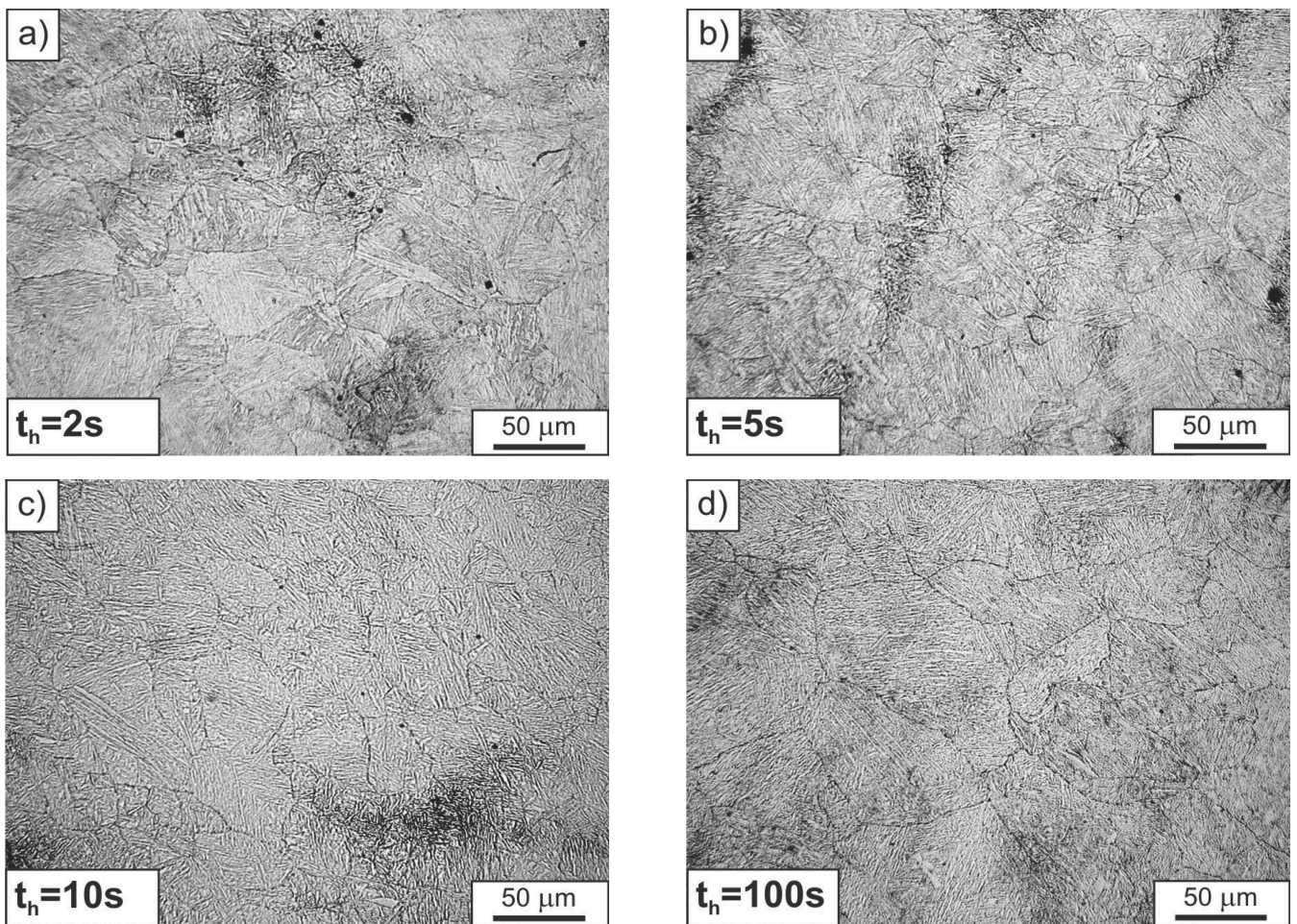


Fig. 14. Primary austenite grains of steel B revealed after two-stage compression tests at the temperature of 1000°C at the rate of 10 s<sup>-1</sup> applying breaks between deformation steps in a range from 2 s to 100 s (a-d)

While experimentally determined values of  $t_{0.5}$  for the B steel reveal good correspondence with the model dependence (3). Comparison of model and experimental values of the  $t_{0.5}$  time for the A and B steel is presented in Table 4.

Table 4.

The comparison of measured and calculated values of  $t_{0.5}$  time

Steel	Temperature of plastic deformation	Values of $t_{0.5}$ time, s	
		experimental	calculated
A	1100	6.0	5.8
	1000	10.0	15.5
	900	30.0	33.0
B	1100	8.0	12.9
	1000	20.0	20.2
	900	65.0	62.0

Large austenite grains with average diameter of 64 μm, after static recovery occurring in the time equal 2 s, were revealed in the microstructure of the A steel, deformed in two stages at the temperature of 900°C. After isothermal holding at the temperature of 900°C for 5 s there is a decrease of the rate of the course of

thermally activated processes, connected most likely to formation of nuclei of static recrystallization. Isothermal holding of the A steel specimens at such temperature for 10 s leads to the initial stage of static recrystallization, wherein in these conditions the degree of softening (decay of strain hardening) is equal  $X=0.32$ . Increase of isothermal holding time up to 100 s ( $X=0.83$ ) results in grain growth of austenite. Distinct refinement of primary austenite grain in comparison to the initial state, caused probably by partial course of dynamic recrystallization during deformation and the course of metadynamic and static recrystallization after deformation was observed after two-stage compression of the A steel at the rate of 10 s<sup>-1</sup>, at the temperature of 1000 and 1100°C. Isothermal holding after deformation of the A steel specimens at the temperature of 1000°C for 2 and 5 s leads to obtaining 23% and 32% fraction of recrystallized austenite, respectively and the size of the phase of 32 μm and 22 μm, respectively. Slowing down of the process of decay of hardening is observed after isothermal holding at the temperature of 1000°C for 10 s, what is connected with formation of nuclei of static recrystallization. Austenite grain size after isothermal holding of specimens for 10 s

is equal approximately 16  $\mu\text{m}$ , and the recrystallized fraction is equal to 50%. The progress of recrystallization process and growth of  $\gamma$  phase grains is observed for the time of isothermal holding equal 50 and 100 s. Isothermal holding of samples for 50 s leads to obtaining 84% fraction of recrystallization and mean diameter of austenite grains of approx. 35  $\mu\text{m}$ . Increase of time up to 100 s results in obtaining microstructure characterized with 95% fraction of recrystallization and average diameter of  $\gamma$  phase grain size equal 78  $\mu\text{m}$ . Decrease of hardening of the A steel after double-hit compression at the temperature of 1100°C is determined by the course of dynamic recrystallization after isothermal holding of samples at this temperature for 2 and 5 s, and successively, by the course of static recrystallization for the time of holding equal to 10, 50 and 100 s.

The size of primary grains of austenite varies from about 27  $\mu\text{m}$  for holding time of 2 s, to about 63  $\mu\text{m}$  for holding time equal 100 s. In the result of two-stage compression of the B steel at the temperature of 900°C, at the rate of 10  $\text{s}^{-1}$ , diversified grain size of primary austenite, in a range from 25  $\mu\text{m}$  to 70  $\mu\text{m}$ , was obtained in a consequence of static recovery and static recrystallization. Two-stage deformation of the B steel at the temperature of 1000°C with the use of isothermal holding for the time equal from 2 s to 100 s caused a decrease of strain hardening as a result of the course of static recovery (Fig. 14a) and static recrystallization (Figs. 14b-d). In the examined range of isothermal holding, average diameter of austenite grains varies from 14  $\mu\text{m}$  to 60  $\mu\text{m}$ , and obtained decrease of hardening is equal  $X=0.83$ . Isothermal holding of specimens at the temperature of 1100°C for 2 and 5 s after first stage of deformation equal  $\varepsilon=0.2$  caused a decrease of hardening of steel as a result of the course of static recovery and static recrystallization which determines obtaining primary austenite grains with mean diameter of 20  $\mu\text{m}$  and 33  $\mu\text{m}$ , respectively. The recrystallized fraction of for isothermal holding time of 10, 50 and 100 s is equal to 63%, 83% and 96%, respectively.

#### 4. Conclusions

Continuous compression tests of investigated steels performed at the strain rate of 1, 10 and 50  $\text{s}^{-1}$  allowed to determine the influence of plastic deformation temperature in a range from 1100 to 900°C on the shape of  $\sigma$ - $\varepsilon$  curves and  $\varepsilon_m$  strain, corresponding to maximum value of flow stress, and hence to estimate strain necessary to initiate dynamic recrystallization of austenite. Analysis of flow curves of studied steels indicates that the increase of strain rate from 1 to 50  $\text{s}^{-1}$  causes the increase of the maximum value of flow stress, by the average of 50 MPa, regardless of applied temperature. Obtained values of activation energy indicate that the process of plastic deformation of studied steels is controlled by dynamic recrystallization.

Performed two-stage compression tests revealed, that apart from the temperature, considerable influence on kinetics of recovery and static recrystallization is exerted by chemical and phase composition of steel after hot-working is concluded and that the  $t_R$  time of total recrystallization of steel containing microadditions of elements with high chemical affinity for carbon and nitrogen, bounded in dispersive particles of carbides, carbonitrides or nitrides at recrystallization temperature, is long. Determined time of total recrystallization of austenite,  $t_R$ , in

a temperature range from 1100°C to 900°C changes from 100 to 600 s and from 300 to 800 s - for the Ti-V steel and Ti-Nb-V steel, respectively. It means that the complete recrystallization of austenite requires long times, unacceptable in a production process of forgings. Therefore, the  $t_{0.5}$  time has a greater meaning than  $t_R$  for technological purposes. Moreover, considerable deformation at high rate and short intervals for moving produced parts from one die to another do not create convenient conditions for the course of static recrystallization, allowing grain refinement of austenite. Hence, forgings should be isothermally held at a temperature of forging finish prior to hardening for the time necessary to form about 50% fraction of recrystallized austenite, which for the A steel is equal 30 s, and 65 s for the Nb-containing steel. Lower rate of static thermally activated processes in the B steel in relation to the A steel is a result of the presence of Nb microaddition, which being formed on dislocations during plastic deformation in a form of dispersive NbC carbides, slows down the course of recovery and dynamic recrystallization, and after hot-working is done, decreases the rate of recovery and static recrystallization and limits grain growth of recrystallized austenite.

#### Acknowledgements

Scientific work was financed from the science funds of the Polish Ministry of Science and Higher Education in a period of 2010-2013 in the framework of project No. N N508 585239.

#### References

- [1] A. Ghosh, S. Das, S. Chatterjee, B. Mishra, P. Ramachandra, Influence of thermo-mechanical processing and different post-cooling techniques on structure and properties of an ultra low carbon Cu bearing HSLA forging, *Materials Science and Engineering A348* (2003) 299-308.
- [2] D.K. Matlock, G. Krauss, J.G. Speer, Microstructures and properties of direct-cooled microalloy forging steels, *Journal of Materials Processing and Technology* 117 (2001) 324-328.
- [3] P. Skubisz, H. Adrian, J. Sińczak, Controlled cooling of drop forged microalloyed-steel automotive crankshaft, *Archives of Metallurgy and Materials* 56/1 (2011) 93-107.
- [4] D. Jandová, R. Divišová, L. Skálová, J. Drnek, Refinement of steel microstructure by free-forging, *Journal of Achievements in Materials and Manufacturing Engineering* 16/1-2 (2006) 17-24.
- [5] J. Adamczyk, M. Opiela, Engineering of forged products of microalloyed constructional steels, *Journal of Achievements in Materials and Manufacturing Engineering* 15/1-2 (2009) 159-165.
- [6] J. Sińczak, J. Majta, M. Głowacki, M. Pietrzyk, Prediction of mechanical properties of heavy forgings, *Journal of Materials Processing and Technology* 80-81 (1998) 166-173.
- [7] A. Grajcar, R. Kuziak, Softening kinetics in Nb-microalloyed TRIP steels with increased Mn content, *Advanced Materials Research* 314-316 (2011) 119-122.

- [8] W. Ozgowicz, M. Opiela, A. Grajcar, E. Kalinowska-Ozgowicz, W. Krukiewicz, Metallurgical products of microalloy constructional steels, *Journal of Achievements in Materials and Manufacturing Engineering* 44/1 (2011) 7-34.
- [9] T. Gladman, *The Physical Metallurgy of Microalloyed Steels*, The Institute of Materials, London, 1997.
- [10] J. Adamczyk, Development of the microalloyed constructional steels, *Journal of Achievements in Materials and Manufacturing Engineering* 14/1-2 (2006) 9-20.
- [11] H.L. Andrade, M.G. Akben, J.J. Jonas, Effect of molybdenum, niobium, and vanadium on static recovery and recrystallization and on solute strengthening in microalloyed steels, *Metallurgical Transactions* 14A (1983) 1967-1977.
- [12] J. Adamczyk, *Engineering of Metallic Materials*, Silesian University of Technology Publishers, Gliwice, 2004 (in Polish).
- [13] S.F. Medina, M. Gómez, P.P. Gómez, Effect of V and Nb on static recrystallization of austenite and precipitate size in microalloyed steels, *Journal of Materials Science and Technology* 45 (2010) 5553-5557.
- [14] A. Grajcar, Structural and mechanical behavior of TRIP-type microalloyed steel in hot-working conditions, *Journal of Achievements in Materials and Manufacturing Engineering* 30/1 (2008) 27-34.
- [15] C.M. Sellars, Proceedings of the International Conference "HSLA Steels'85", Chinese Society of Metals, Beijing, 1985, 12-22.
- [16] M. Opiela, Analysis of the kinetics of precipitation of MX-type interstitial phases in microalloyed steels, *Journal of Achievements in Materials and Manufacturing Engineering* 47/1 (2011) 7-18.